International Journal of Heat and Mass Transfer 92 (2016) 1171–1181

Contents lists available at ScienceDirect

International Journal of Heat and Mass Transfer

journal homepage: www.elsevier.com/locate/ijhmt

Effect of vapor flow on the falling film evaporation of R134a outside a horizontal tube bundle

Wen-Tao Ji [a], Chuang-Yao Zhao [a], Ding-Cai Zhang [a], Shun Yoshioka [b], Ya-Ling He [a], Wen-Quan Tao [a,*]

[a] Key Laboratory of Thermo-Fluid Science and Engineering of MOE, School of Energy and Power Engineering, Xi'an Jiaotong University, Xi'an 10049, China
[b] Environmental Technology Laboratory, Daikin Industries, Ltd., Osaka 591-8511, Japan

ARTICLE INFO

Article history:
Received 13 April 2015
Received in revised form 7 September 2015
Accepted 8 September 2015

Keywords:
Falling film evaporation
Heat transfer
Refrigerant
Tube bundle

ABSTRACT

The effect of vapor flow on the falling film evaporation of refrigerant R134a outside a horizontal tube bundle is investigated with an experimental approach. The test space is a cube with a rectangular cross section of 0.575 m (length) × 38.8 mm (width). The tube bundle was 3 × 6 (columns × rows) of staggered horizontal finned tubes made of copper. The longitudinal tube pitch is 22.5 mm and the transverse is 19.9 mm. The external fin density of test tube is 45 fpi (fins per inch), and outside diameter is 19.05 mm. The vapor flow velocity can be adjusted in the range of 0–3.1 m/s. Liquid falling film flow rate ranges from 0.07 to 0.2 kg/m·s. Experiment is firstly conducted at saturation temperature of 6 °C without the effect of additional vapor flow at the heat flux of 20, 60, 100 and 180 kW/m^2 (for the first tube row). Vapor flow effect experiment was carried out at three heat fluxes 20, 40 and 60 kW/m^2. It is found that falling film flow rate is an important factor to influence the evaporating heat transfer coefficient. With the effect of vapor flow, both positive and negative effects are observed as the increment of vapor velocity. Positive effects are predominant for the two tubes in the top positions and higher vapor velocity.

1. Introduction

Falling film evaporation is a cost-effective heat transfer enhancement techniques. It can be operated with lower temperature difference and refrigerant consumption. In the recent decades, it has been gradually used in refrigeration and air-conditioning systems. Many experimental investigations have been conducted on the falling film evaporation of refrigerant [1–3]. Comprehensive reviews were provided by Thome [4], Ribatski and Jacobi [5], Fernández-Seara and Pardiñas [6], and Abed et al. [7]. Compared with flooded evaporators in the air conditioning systems, the advantages of falling film evaporators generally include the following three aspects: (1) higher heat transfer coefficient. The saturate temperature of evaporator and system efficiency were increased to provide higher refrigeration capacity; (2) Charging amount of refrigerant will be reduced. The operating costs of the system and the potential pollution of refrigerant on the environment will also be reduced. (3) Lubricant is easy to be recovered from the evaporator. For the flooded evaporator, the lubricant is miscible with refrigerant, which is difficult to separate and will influence the boiling heat transfer coefficient. These three advantages make the falling film evaporator having great potentials in refrigeration and air-conditioning industry. However, the system for falling film evaporation is comparably complicated. It involves many influencing factors, such as liquid distribution, tube alignment, film liquid flow rate. In addition, the experimental conditions are more difficult to reproduce and repeat. For these reasons, well-accepted research results and experimental data on the falling film evaporation heat transfer are still quite limited. To the author's knowledge, no benchmark data so far were obtained for the falling film heat transfer of refrigerants. Large deviations still exist between the data from different authors. For example, in the experimental result of Moeykens [8] at T_s = 2 °C, the falling film heat transfer coefficients of R134a outside plain tube at heat flux of 0–40 kW/m^2 ranged from 1.5 to 4.5 kW/m^2·K, while the experiment result of Gstoehl [9], Roques and Thome [10] ranged from 9 to 14 kW/m^2·K in the same heat flux range at T_s = 5 °C.

Following is a brief literature review on the falling film (or spray) evaporation of refrigerant outside the horizontal tube bundle.

Falling film evaporation of R134a, R22 and R123 outside horizontal, plain and finned (40 fpi, fins per inch) tube bundles were studied by Moeykens [8] and Moeykens and Pate [11] in 1994. The tubes used in the experiment were made by copper with diameters of 12.7 mm and 19.1 mm. The finned tubes include GEWA-SC, Turbo-B and Turbo-CII, which were heated electrically by inserted

* Corresponding author. Tel.: +86 29 82669106.
E-mail address: wqtao@mail.xjtu.edu.cn (W.-Q. Tao).

http://dx.doi.org/10.1016/j.ijheatmasstransfer.2015.09.023
0017-9310/

Nomenclature

A	area, m^2
c_i	enhanced ratio of inside heat transfer coefficient
c_p	specific heat capacity, $J \cdot kg^{-1} \cdot K^{-1}$
d	diameter of tube, mm
e	height of outside fin, mm
h	heat transfer coefficients of heat surface, $W \cdot m^{-2} \cdot K^{-1}$
H	height of inside fin
k	overall heat transfer coefficients, $W \cdot m^{-2} \cdot K^{-1}$
L	tube's tested length, m
m	mass flow rate, $kg \cdot s^{-1}$
Pr	Prandtl number in Gnielinski's equation
q	heat flux, $W \cdot m^{-2}$
Re	Reynolds number
R_w	thermal resistance of tube wall
t	external fin thickness, mm
T	temperature, °C

Greek alphabet

ϕ	heat transfer rate, W
λ	thermal conductivity, $W \cdot m^{-1} \cdot K^{-1}$
Γ	falling film flow rate per unit length, $kg \cdot m^{-1} \cdot s^{-1}$
ΔT_m	logarithmic mean temperature difference
η	dynamic viscosity, $N \cdot s \cdot m^2$

Subscript

a	average
c	cooling
e	evaporating
i	inside of tube
in	inlet of tube
m	number of tubes fixed in the evaporator
n	number of tubes fixed in the condenser
o	outside of tube
out	outlet of tube
p	pump
s	saturation
w	wall

cartridge heaters. The heat flux ranged from 5 to 40 kW/m^2. Pool boiling experiments were also performed with the same tube bundles and the results were compared with spray evaporation under similar conditions. It was found that the heat transfer performance for spray evaporation was greater than the pool boiling performance measured on the same tube. The enhanced Turbo-CII tube, which is designed for condensation, the heat transfer coefficient up to 100% higher than those of GEWA-SC was reported. It was also observed that the falling film evaporation heat transfer coefficient was significantly affected by the liquid feed rate only when dry-out occurs.

Under adiabatic flow conditions, visualizations of falling film outside four types of tubes have been reported by Roques et al. [12] and Gstöhl and Thome [13] with three different fluids. The enhanced tubes include low finned tube Turbo-Chil, boiling tube Turbo-BII and condensation tube Thermoexcel-C. At low flow rates, the flow mode was discrete falling droplets. With the increment of flow rate, liquid columns and continuous sheet of liquid were observed subsequently. Based on the visualization results, correlations to predict the flow mode transitions between droplet, column and sheet flows were presented for the four tubes. Although the heat transfer condition is different from the adiabatic experiment, the investigation helps to understand the general distribution of liquid film under different flow rate.

Ribatski and Thome [14] tested the falling film evaporation of refrigerant R134a on five commercial tubes. The tubes include a plain tube, two enhanced boiling tubes (Turbo-BII HP and Gewa-B), one enhanced condensing tube (Turbo-CSL) and a porous coated tube (High-flux). Experiments were conducted at saturation temperatures of 5, 10 and 20 °C, nominal heat fluxes of 20, 40 and 60 kW/m^2. The film flow rates ranged from 0.02 kg/m·s to 0.25 kg/m·s on an array of 6–10 tubes. It was observed that small dry region area on the tube surfaces did not necessarily causing a decrease in the heat transfer coefficient, and only a predominance of dry regions on the surface would lead to a decrease in the heat transfer coefficient. The vapor flow effect was also tested with transparent plates configured laterally at both sides of the tube row. Each plate was 3 mm away from the tube bundle. For quiescent vapor and concurrent vapor flow, it did not affect the liquid flow distribution and heat transfer performance within their test range. The vapor velocity was within 1.0 m/s between the tube and plate clearance.

Falling film heat transfer of R134a on different horizontal tube bundles was investigated by Roques and Thome [1,10]. The tubes in the experiment include plain, Turbo-BII HP, Gewa-B and High-flux. Modified Wilson plot method was adopted to separate the evaporating heat transfer coefficient from overall thermal resistance. The evaporating heat transfer coefficients of Turbo-BII HP were in the order of 25 $kW/m^2 \cdot K$ at heat flux 40 kW/m^2. High-flux tube gives the highest heat transfer performance among the four tubes. The heat transfer coefficient was around 60 $kW/m^2 \cdot K$ at heat flux 49.7 kW/m^2. The falling film heat transfer coefficient on plain tube was 40% higher than pool boiling at heat flux 40 kW/m^2. The average pool boiling and falling film heat transfer coefficients were respectively of 9160 and 13000 $W/m^2 \cdot K$. A heat transfer plateau was obtained when overfeed film flow rate was large enough that dry-out condition did not occur. A new predictive method was also developed. It predicted most of the current local heat transfer coefficient for R-134a within ±20% for conditions without dry-out.

Ruan et al. [15] tested the effect of countercurrent air flow on the falling film mode transitions between horizontal tube bundles. The liquids in the experiment were water and ethylene glycol. An open wind tunnel with a blower was used to create an upward gas flow as the liquid falls from the tube bundle. The liquid distributor was made by a combination of tube and Plexiglas box all with perforating holes in the bottom. Through the distributor, the liquid was distributed uniformly outside the tube bundles under adiabatic flow conditions. The wind tunnel intersected with the tube bundle. Experiments were conducted at several fixed blower speeds. The water mass flow rate per unit length reached up to 0.3 kg/m·s, and gas velocity reached about 6 m/s. With the increase of vapor velocity, the falling film gradually becomes more unsteady. When the gas flow velocity was larger than 3.5 m/s, steady mode was disturbed and the mode classification was difficult. Only the adiabatic condition was tested in the experiment.

Christians and Thome [2,3] tested the falling film and pool boiling heat transfer of R134a and R236fa on a single vertical row of horizontal tubes. Enhanced boiling tubes, Turbo-B5 and Gewa-B5, were tested at saturate temperature 5 °C. The film Reynolds numbers ranged from 0 to 3000, and heat flux was between 15 and 90 kW/m^2 in both pool boiling and falling film heat transfer conditions. It was found that R134a outperformed R236fa outside the two tubes. The heat flux had less effect on the falling film heat

transfer compared with pool boiling. The experiment also indicated that at lower heat flux less than 20 kW/m^2, thermocouples were nearing the limits of their applicability; it might approach the resolution limit of thermocouples.

As indicated above, when the falling films flow rate is lower than a threshold, a significant decrease in the heat transfer performance will be observed. How to prevent dry-out is most important and need to be consciously considered. The flow of vaporized fluid can be detrimental. It significantly expands in volume and the film can be easily blown away before contacting the tube surface. The tubes in lower position might not be able to contact with sufficient liquid film, dry-out occurs and the efficiency of falling film evaporator may reduce compared with flooded evaporator. For this reason, more reliable data on the effect of vapor flow in the falling film heat transfer is desirable for engineering design purpose.

In this paper, experimental results on the effect of vapor flow on the falling film evaporating of R134a outside six horizontal tubes are presented. In the experiment, R134a vapor flow is distributed uniformly from the bottom of tube array to the test section. Vaporized fluid is in a direction that is opposite to the flowing direction of liquid fluid under the effect of gravity.

The rest of the paper is organized as follows. In Section 2, experimental apparatus is introduced, including the test loop and the specific structure of test section. Then the test procedure is presented in Section 3. Section 4 is the data reduction method and the uncertainty analysis. The measurement results and discussion are provided in Section 5. Finally some conclusions are summarized in Section 6.

2. Experimental apparatus

The experimental apparatus consists of three cycles: refrigerant, heating and cooling water circulating system. The schematic diagram of the test apparatus and the three cycles are shown in Fig. 1.

Liquid R134a is firstly charged in the condenser, and then pumped to the evaporator by canned motor pump. Before entering the evaporator, refrigerant flow is divided into two branches. One branch is flowing across an electric heating boiler, where the liquid refrigerant is heated and converted to vapor, then flows to the test section. The heating power of boiler can be adjusted as needed. The vapor is distributed uniformly from the bottom of tube bundle. Another branch directly flows to the liquid distributor in the top of test section and the liquid refrigerant film is distributed outside the horizontal tube bundle. The refrigerant evaporates when flowing through outside of the test tube bundle, where the heating water flows through the inside of test tube bundle. The liquid refrigerant that does not evaporate will returns to the refrigerant storage tank from the bottom of evaporator by gravity.

The vapor from evaporator is collected and flows into the condenser. The vapor is condensed outside the condensing tube bundle fixed in the condenser. This is the circulation of refrigerant. The liquid is stored in the bottom of condenser, the top part of which is mounted with condensing tubes. Sub-cooling tubes are also installed in the bottom of condenser. The refrigerant circulating flow rate is measured with Siemens MASS2100 Coliolis mass flow meter (the error is within ±0.1% in the whole measurement range). The whole apparatus is enwrapped with rubber plastic of

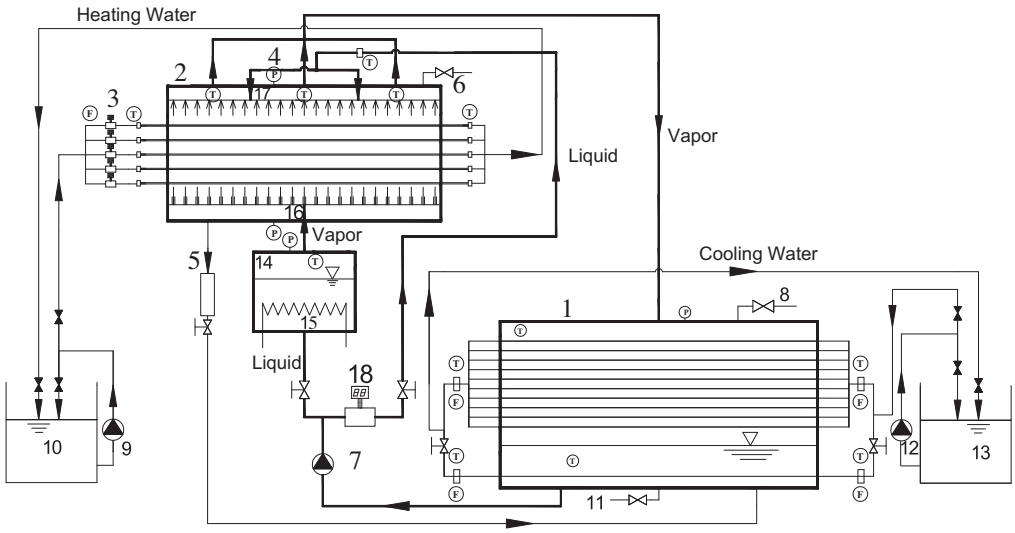

(1) Condenser and refrigerant storage tank; (2) Falling film evaporator and the test section;

(3) Electromagnetic flow meter; (4) Pressure gauge; (5) Condensate measuring container;

(6) Exhausting valve; (7) Canned motor pump; (8) Refrigerant charging valve; (9) Hot water pump;

(10) Hot water tank; (11) Refrigerant outlet; (12) Cooling water pump; (13) Cooling water tank;

(14) Auxiliary vapor generator and the boiler ; (15) Electric heater; (16) Vapor distributor;

(17) Liquid distributor; (18) Coliolis mass flow meter

Fig. 1. Schematic diagram of experimental apparatus.

thickness 40 mm for insulation; and the rubber plastic is coated with aluminum foil to prevent the heat loss or input from the environment.

The test section in the evaporator has a length of 575 mm, width 38.8 mm and height 450 mm. The tube bundle is fixed in the evaporator. The bundle distance, tube position and tube diameter can be different according to the experimental purposes. The vessels and flanges are made by stainless steel. The power of boiler can be adjusted from 0 to 40 kW. Dynamometer with the accuracy of 40 W is used to record the power. The external diameter and the length of electric heating boiler are 406 mm and 1000 mm, respectively. A special vapor distributor is designed to release vapor from boiler to the test section. The thickness of boiler wall is 10 mm. The pressure is measured independently. The temperature is monitored with two Pt100 transducers with an accuracy of ±0.15 °C. One copper pipe channel with internal diameter of 16 mm is welded in the vessel and transmits the vapor to the evaporator. For the circulation of refrigerant, a condenser is needed. The condensing vessel in the apparatus has an internal diameter of 450 mm and 1140 mm in length.

The heating water and cooling water are operated in two independent circulations. The heating water flows through the inside of test tube bundle, and returns to the hot water tank. The hot water tank is a thermostatic water bath, the temperature of which can be adjusted in the range of 10–60 °C. The cooling water flows through the condensing tubes fixed in the condenser. The cooling water tank is also a thermostatic water bath, the temperature of which can be adjusted in the range of 2–60 °C. The hot water tank and the cooling water tank both have the independent refrigerant and electric heating systems. The volumes of two tanks are both 3 m^3. The temperatures and flow rates are measured independently with transducers (Thermal couples and Siemens MAG5100W electromagnetic flow meters (Error is within 0.1% in the whole measurement range)).

Two pressure gauges are used to monitor the pressure of evaporator; the tested range is from 0 to 2.5 MPa, which has the precision of ±0.00625 MPa. Seven platinum temperature transducers (Pt100), with a precision of $\pm(0.15 \pm 0.002|t|)$K, are configured in different part of the evaporator, boiler and condenser to measure the vapor and liquid temperatures of the refrigerant; the temperature of refrigerant film is measured before it getting into the liquid distributor with one Pt100. The temperature and temperature difference of water flows through each evaporating or condensing tube are measured by thermal couples and five-junction copper-constantan thermocouple piles, respectively. The thermocouples and thermocouple piles were all calibrated against a temperature calibrator that has the precision of ±0.2 K. The electric potential of thermocouple and thermocouple piles are measured with Keithley 2700 digital voltmeter, which has the resolution of ±0.1 μV. The specifications of the test tubes is given in Table 1, where d_o is the diameter of the embryo tube.

The test tube is originally designed for enhancing pool boiling heat transfer, which has an external fin density of 45 fpi (fins per inch), 0.574 mm in the fin height and the outside diameter is 19.05 mm (see Table 1 and Fig. 2). Two flanges with 8 tube openings are designed to fix the test tubes. The tubes are fixed in the flange through tube expander. Six enhanced tubes are positioned in the top. Two smooth tubes are in the bottom for validation and avoid the direct contact of vapor flow from the distributor and test tubes. The longitudinal tube pitch is 22.5 mm and the transverse is 19.9 mm. The center column is for test and two side columns of half tubes are made by transparent glass to simulate the experimental condition of falling film evaporator (see Fig. 3). The transverse narrowest bundle clearance is 3.25 mm where the vapor velocity can be regulated in the range of 0–3.1 m/s (calculated from the bottom of tube bundle's narrowest clearance) by changing the electric heating power of boiler.

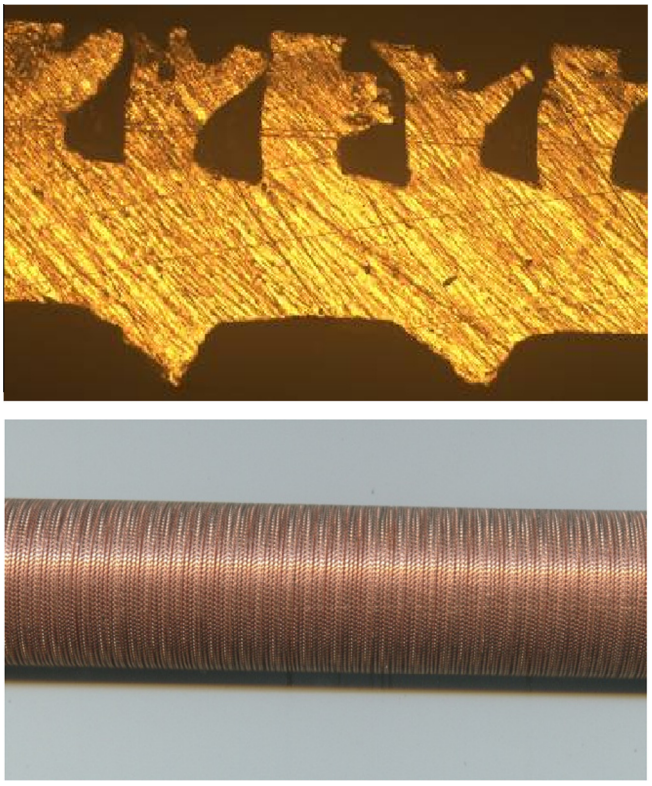

Fig. 2. Cross sections of tube No. 1.

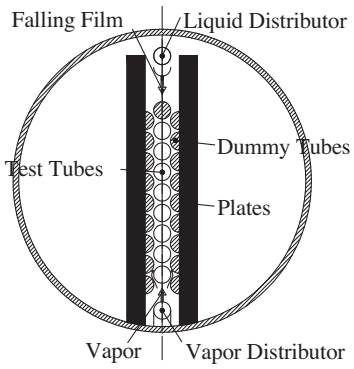

Fig. 3. Schematic diagram of test section.

Table 1
Specifications of tested tubes.

Tubes	Outside diameter d_o (mm)	Inside diameter d_i (mm)	Height of outside fin e (mm)	Outside fin numbers per inch	External fin thickness t (mm)	Height of inside fin H (mm)	Length of test section L (mm)
Plain	19.17	16.40	–	–		–	1540
No.1	19.05	16.70	0.574	45	0.336	0.320	575

The test section is composed of test tubes, half glass tubes and the glass plates, which is all fixed in the evaporator. The half tubes made by glass are pasted tightly inside two glass plates without clearance. Through the glass, the liquid distribution and fluid flow inside the test section can be observed. The vapor flows out from the top of the test section. In the bottom of the test section, one channel is connected to the bottom of the liquid storage tank. The tank has certain liquid level, so, the vapor cannot flow out from this channel. Only the un-vaporized fluid flows into the liquid storage tank.

3. Experimental procedure

After the test tubes are fixed in the evaporator, the system is charged with nitrogen to the pressure of 1.2 MPa to check the tightness of the system. After all the leaks are eliminated, the pressure of the system is kept at least 24 h, and the high pressure nitrogen is discharged. Then, the system is evacuated by a vacuum pump to an absolute pressure of at least 1500 Pa. Keep this degree of vacuum for at least 8 h. If no leak is detected, then the refrigerant R134a is charged into the system through the valve installed on the top of condenser.

A small amount of liquid refrigerant is firstly charged into the system, then evacuates with a vacuum pump. Repeat this process for at least four times until the none condensable gases in the system is reduced to a minimum amount. Finally, the refrigerant is charged into the liquid refrigerant storage tank.

In the experiment, the difference between the temperature of liquid refrigerant before the film distributor and the one corresponding to the measured pressure according to the thermodynamics table is within 0.2 K [16]. If the difference of the two temperatures is not within 0.2 K, the vapor refrigerant is exhausted by the valves fixed in two ends of condenser and evaporator to meet this requirement.

Before taking each experimental data, at least 3 h is waited until the system reaches the steady state. After the experimental system is in a steady state, the test data are recorded. The steady state is characterized by (1) the variation of the required saturation temperature of refrigerant is in the allowed range, usually ±0.05 K of directly Keithley voltmeter monitored result, and (2) the fluctuation of water temperature at inlet and outlet of condenser and evaporator was within ±0.1 K, mostly within ±0.05 K.

4. Data reduction

From the measured quantities, energy balance of the system is examined by the following equations.

Heating power input from heating water:

$$\phi_{e,m} = \dot{m}_{e,m} c_{p,m} \left(T_{e,m,in} - T_{e,m,out}\right) \tag{1}$$

Cooling power output from cooling water:

$$\phi_{c,n} = \dot{m}_{c,n} c_{p,n} \left(T_{c,n,out} - T_{c,n,in}\right) \tag{2}$$

In the two equations above, $T_{e,m,in}$, $T_{e,m,out}$ are the inlet and outlet temperatures (K) of heating water, respectively, for the m^{th} tube, $T_{c,n,in}$, $T_{c,n,out}$ are the inlet and outlet temperatures (K) of cooling water for the n^{th} tube, respectively, $c_{p,m}$ and $c_{p,n}$ are the specific heat capacity of heating and cooling water, respectively, corresponding to the mean temperature of inlet and outlet water ($J \cdot kg^{-1} \cdot K^{-1}$), and $m_{e,m}$, $m_{c,n}$ are the mass flow rates of heating and cooling water (kg/s), respectively. m and n are the number of heat exchanging tubes fixed in the evaporator and condenser, respectively.

The heat balance requirement is:

$$\frac{\left|\left(\sum_{m=1}^{k} \phi_{e,m} + \phi_p\right) - \sum_{n=1}^{l} \phi_{c,n}\right|}{\phi_a} \leqslant 3\% \tag{3}$$

In the equation, ϕ_p is the power of canned motor pump, 1.5 kW, by which the refrigerant is pumped into the evaporator. For all data recorded, the heat balance should be less than 3% in most circumstances, 5% at most.

In Eq. (3), ϕ_a is the mean heat transfer rate of tube bundle:

$$\phi_a = 0.5\left(\sum_{m=1}^{k} \phi_{e,m} + \sum_{n=1}^{l} \phi_{c,n} + \phi_p\right) \tag{4}$$

Overall heat transfer coefficient of each test tube is determined with the following equation:

$$k = \frac{\phi_{e,m}}{A_o \Delta T_m} \tag{5}$$

where,

$$A_o = \pi d_o L \tag{6}$$

ΔT_m is the log-mean temperature difference of each test tube in experiment:

$$\Delta T_{m,m} = \frac{\left|T_{w,m,in} - T_{w,m,out}\right|}{\ln\left(\frac{T_s - T_{w,m,in}}{T_s - T_{w,m,out}}\right)} \tag{7}$$

From the overall heat transfer coefficient k, the outside falling film evaporating heat transfer coefficient h_o is obtained with the following equation:

$$\frac{1}{h_o} = \frac{1}{k} - \frac{A_o}{A_i}\frac{1}{h_i} - R_w \tag{8}$$

In Eq. (8), A_i is the area of inner tube wall, R_w is the thermal resistance of the tube wall, and h_i is water side heat transfer coefficient, determined by the Gnielinski equation [17]. If the internal surface is enhanced by grooves, Wilson plot is adopted to obtain the water side heat transfer coefficient [18]. In order to reduce the uncertainty of h_o in the experiment, the thermal resistance in the tube side is mostly higher than shell side. Furthermore, at the higher heat flux greater than 60 kW/m^2, the temperature difference is more than 1 °C and the water velocity in the tube side is increased to at least 3.0 m/s to decrease the thermal resistance of water side.

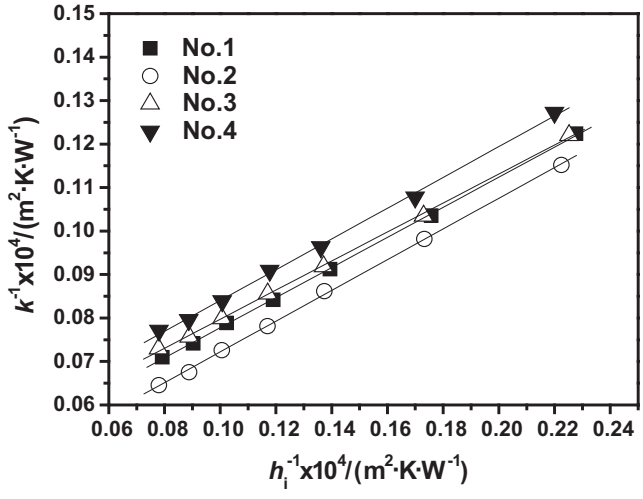

Fig. 4. Wilson plot of four tubes.

Fig. 4 is the Wilson plot of four tested tubes. Internal water velocity is from 0.8 to 3.5 m/s. It shows that the slopes of four tubes are very close to each other. Compared with internal smooth tubes, the enhanced ratios of the four tubes are 3.29, 3.22, 3.41 and 3.21, respectively. As the tubes are manufactured with the same machine and period, so the mean number, 3.28, is used as the enhanced ratio of all the six tubes.

The film Reynolds number is determined by the following equation:

$$\mathrm{Re} = \frac{4\Gamma}{\eta} \tag{9}$$

where Γ is the falling film flow rate per unit length (kg/m·s), which can be measured by Coliolis mass flow meter. η is the dynamic viscosity (N·s/m^2).

Uncertainty analysis is performed according to [16,19]. The confidence level for all measurement uncertainties are 95%. The estimated uncertainties of k are less than 6.2% for all the measurements. As h_o is not directly measured, the uncertainties of h_o is estimated using the method suggested in [19–21]. To calculate h_o, it involves k, h_i and the thermal resistance of tube wall R_w. The uncertainty of heat transfer coefficient on the tube side was claimed as 10% according to [17]. The ratio of the thermal resistance of tube side is less than 55.7%. The worst situation to calculate h_o occurrs when the overall thermal resistance and that of water side thermal resistance are happened to be in an opposite direction. For example, the overall thermal resistance is in a positive direction, and that of water side is in a negative direction. Under such circumstance a maximum error of h_o occurs. The maximum uncertainty of the falling film evaporation heat transfer coefficient, h_o are estimated to be less than 35.2% for all the tubes.

5. Results and discussion

5.1. Validation of the experimental system

When the cooling water is flowing through the plain tubes fixed in the evaporator, heating water is flowing through tubes fixed in the condenser and the refrigerant pump does not work, the experimental apparatus is running in the condensing mode. Refrigerant is boiling in the condenser, rises up to the evaporator, condenses outside the plain tubes, and then flows back to the condenser. Since there is no benchmark data for falling film evaporation in the literature as indicated above, in order to validate our system, the apparatus was firstly operated in the condensing mode in its preliminary test period. The data reduction in condensing mode is described in [22,23], and will not be restated here for simplicity. The data are taken for R134a at saturate temperature 40 °C. The heat flux ranges from 10 to 40 kW/m^2.

Fig. 5 is the comparison of experiment result and Nussellt analytical solution. The deviations are within ±10%. The comparison confirms the reliability of the experimental system.

5.2. Overall falling film heat transfer coefficient without additional vapor flow effect

Experiments are firstly conducted without the effects of additional vapor flow. Fig. 6 shows the overall heat transfer coefficients versus water velocity in the tube side at T_{in} = 10 °C and falling film Reynolds number 2900 (Γ = 0.18 kg/m·s). Pool boiling experiment result on the same tube geometric parameters is also presented for comparison at T_{in} = 12 °C. At the water velocity of 2.5 m/s and heat flux about 42 kW/m^2, the overall heat transfer coefficient is 11.3 kW/m^2·K for falling film evaporation. The corresponding heat transfer coefficient in pool boiling is 9.7 kW/m^2·K at heat flux

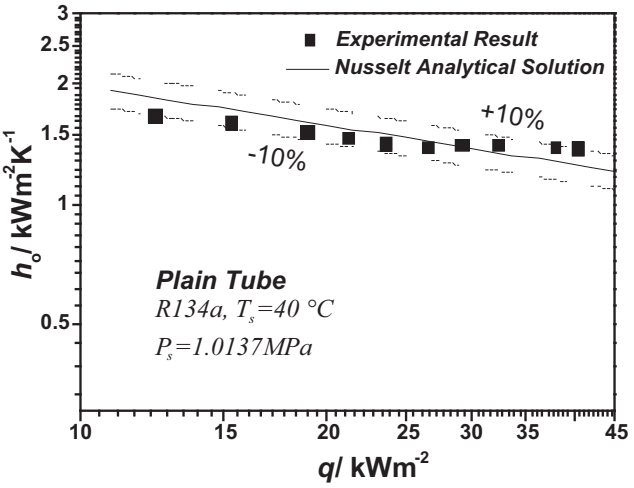

Fig. 5. Comparison of film condensing experiment results with Nusselt analytical solution.

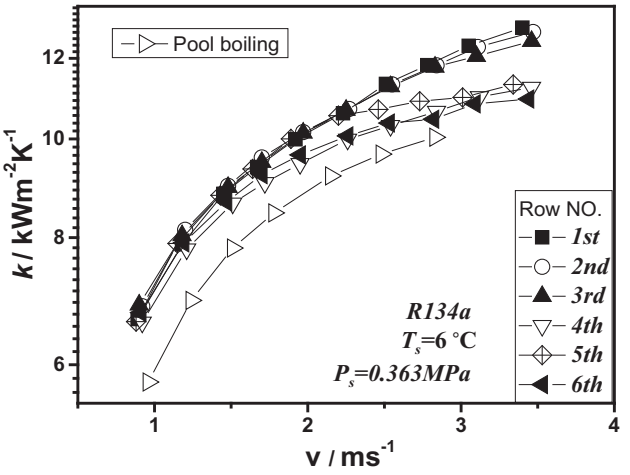

Fig. 6. Overall heat transfer coefficients versus water velocity in the tube side at T_{in} = 10 °C.

about 53 kW/m^2. It is 16% higher than pool boiling. It is also indicated that as the increment of internal water velocity, the heat transfer coefficient in lower positioned tube is lower than the tubes in top position. It is reasonable because the heat transfer coefficient for the higher position is increasing. More liquid film is consumed and the tubes in lowers position can only get less liquid film.

5.3. Falling film heat transfer coefficient without additional vapor flow effect

The experiment without the effect of additional vapor flow is conducted at four fixed heat fluxes 20, 60, 100 and 180 kW/m^2. The heat flux refers to the first tube in the tube bundle. The figures are plotted in the form of h_o versus falling film Re shown in Figs. 7–10. The saturate pressure in the evaporator is 0.363 MPa. The refrigerant temperature from the outlet of distributor is 6 °C, the fluctuation of which is within ±0.1 °C. It should be noted that the vapor shear still exists in the present study with the evaporating of refrigerant outside the tube bundle.

The falling film Reynolds number ranges from 580 to 6400. From the figures, there are three features being observed:

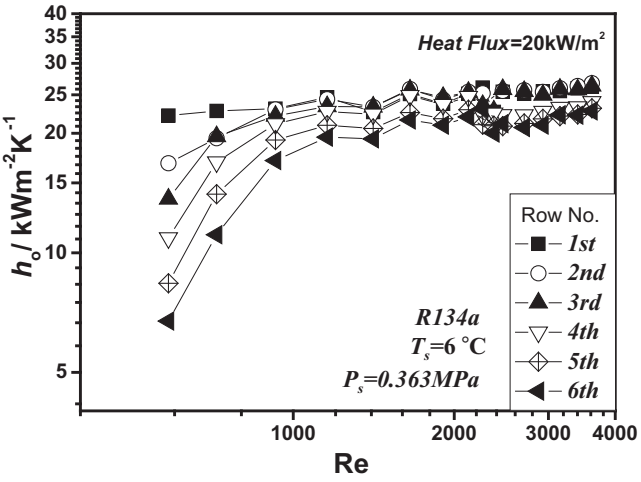

Fig. 7. Falling film heat transfer coefficients versus Re at heat flux of 20 kW/m^2.

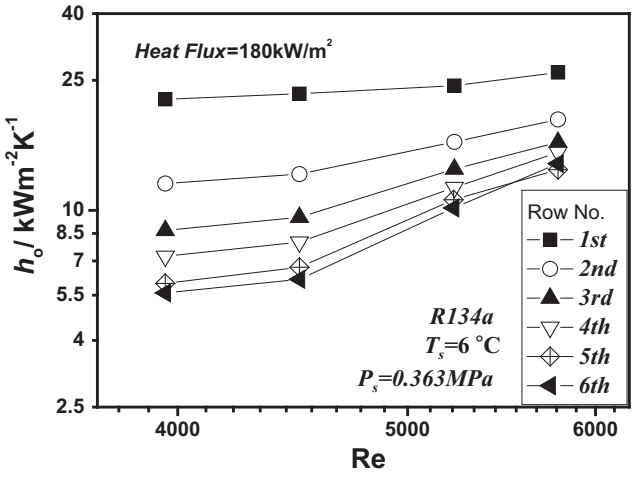

Fig. 10. Falling film heat transfer coefficients versus Re at heat flux of 180 kW/m^2.

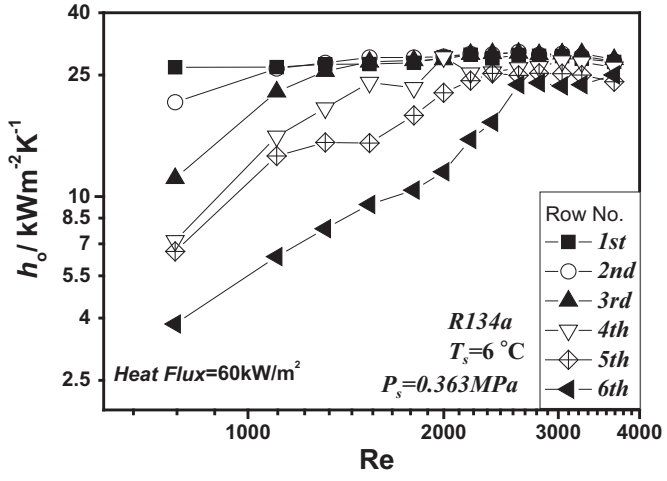

Fig. 8. Falling film heat transfer coefficients versus Re at heat flux of 60 kW/m^2.

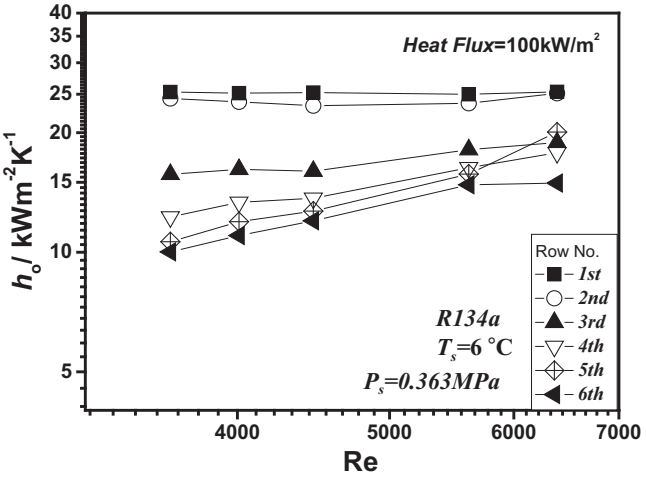

Fig. 9. Falling film heat transfer coefficients versus Re at heat flux of 100 kW/m^2.

(1) For all the four heat fluxes, the 1st tube generally have the highest heat transfer coefficient in the order of 25 kW/m^2·K. At higher heat flux, the heat transfer coefficient of lower position is lower than upper position ranges from 4 to 25 kW/m^2·K. Such large difference in heat transfer coefficients of different row is called bundle effect. It is because the tube in the lower position gets less film flow rate compared with the upper tube positions. As the falling film flow rate decreases, local superheat of the thin film and even dry-out on tube wall may occur, leading to the decrease of heat transfer coefficient. Fig. 11 is the comparison between literature data and present experimental results at heat flux 60 kW/m^2 for the first tube. The tubes include GEWA-C, GEWA-B, GEWA-B4, GEWA-B5, Turbo-B, Turbo-EDE2, Turbo-BII, Turbo-B5, and High flux. As shown in the figure, High flux tube has the highest heat transfer coefficient. The heat transfer performance of GEWA-B5, Turbo-B5 and Turbo-EDE2 is lower than High-flux. The heat transfer coefficient is in the order of 30–40 kW/m^2·K at higher film Re. The other tubes has the lowest heat transfer coefficient in the order of 25 kW/m^2·K.

At lower heat flux 20 kW/m^2 and lower Re, the difference of evaporating heat transfer coefficient are less noted among the vertical arrays; whereas at higher heat flux (60 kW/m^2 and 100 kW/m^2) and lower Re, the difference is very significant. For the higher heat flux, at a fixed Re number, more film evaporates at the upper columns, the lower tube columns get less film, so the heat transfer coefficient difference is significant. It can be expressed by the ratios of h_1/h_m, where m stands for the tube columns. For the 20 kW/m^2 and Re 718, the ratios of h_1/h_2 to h_1/h_6 are respectively of 1.2, 1.2, 1.3, 1.6, and 2.0. For the 60 kW/m^2 and Re of 772, the ratios of h_1/h_2 to h_1/h_6 are respectively of 1.3, 2.3, 3.7, 4.0, and 6.9.

(2) The heat transfer coefficient of different rows increases with Re. At the heat flux of 60 kW/m^2, the heat transfer coefficient of 6th tube row increases from 3825.4 to 25,024.0 W/m^2·K, more than 550%, when Re increases from 772 to 3656. When the heat flux is 100 kW/m^2, at Re of 3625, the heat transfer coefficient of 1st is 2.5 times higher than the 6th tube row; while it is 1.7 at Re of 6400. At the Re of 6400, the difference of heat transfer coefficient among different column is the minimum for all the heat flux.

(3) For the enhanced surface of re-entrant cavity, the heat transfer is enhanced about 38.4–72.3% for the falling film evaporation heat transfer compared with pool boiling (see Fig. 12). The tested tube is designed for pool boiling, which has comparably higher pool boiling heat transfer coefficient

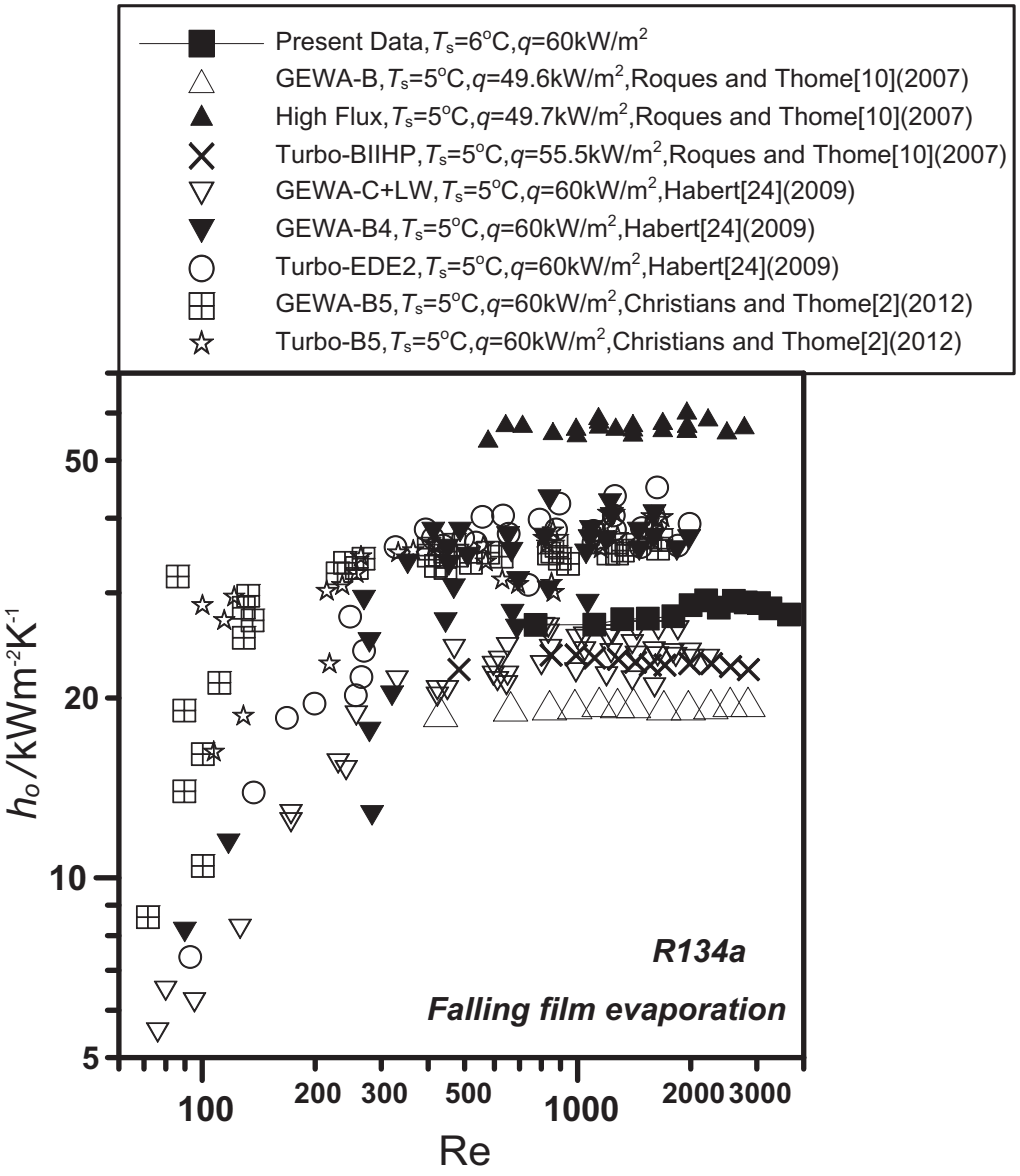

Fig. 11. Comparison between literature data and present experimental result. (See above-mentioned references for further information.)

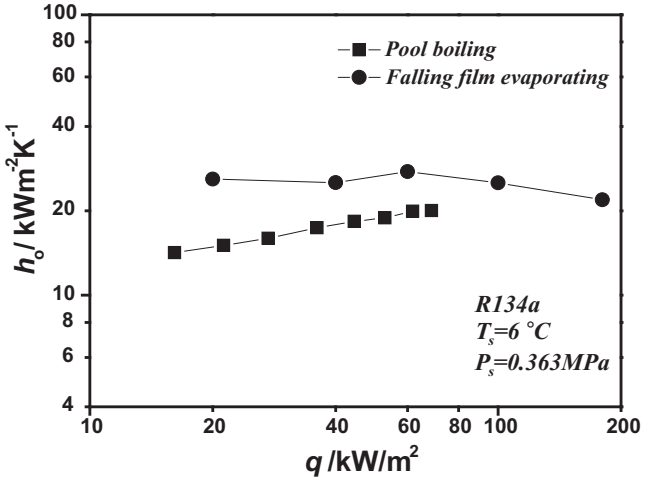

Fig. 12. Comparison of falling film and pool boiling heat transfer coefficients versus heat flux.

according to our previous research [18]. Compared with pool boiling, another feature of the falling film evaporation is that the heat flux has less effect on the heat transfer coefficient. For the 1st tube, the arithmetical average heat transfer coefficient in all Re number for heat flux 40, 60, 100 and 180 kW/m^2 only differ by 16% at most. For the pool boiling heat transfer at the same saturate temperature, in the above heat flux test range the boiling heat transfer coefficient may differ 100% or more.

5.4. Falling film heat transfer experiment result with additional vapor flow effect

Measurements with additional vapor flow effect on the vertical arrays of tubes were performed at the velocity of 0–3.1 m/s and three heat fluxes of 20, 40 and 60 kW/m^2·K. The heat flux also refers to the first tube in the center column of tube bundle. Additional vapor is generated through a electric heating boiler. The electric heating power can be regulated in the range of 0–40 kW. As indicated above, the corresponding vapor velocity in the transverse narrowest bundle clearance 3.25 mm is in the range of

0–3.1 m/s. Additional vapor is designed to distribute uniformly from the bottom of tube array to the test section.

Figs. 13–18 are the falling film evaporation heat transfer coefficient plotted against vapor velocity at falling film flow rate of 0.07, 0.08, and 0.2 kg/m·s and heat flux of 20, 40 and 60 kW/m^2. In Fig. 19, the effects of film Reynolds number on tube heat transfer coefficient at vapor velocity of 3.1 m/s and heat flux of 40 kW/m^2 are presented. From the figures following features should be noted:

(1) The effect of ascending vapor flow on the falling film evaporation heat transfer is very complicated, depending on tube position, falling film flow rate, heat flux and vapor velocity. In the test range studied, tube Nos. 5 and 6 generally have lowest tube heat transfer coefficients. At the same test condition, the tube heat transfer coefficients of the 5th and 6th is only about 1/5–3/5 of that of the first tube. This small heat transfer coefficients are probably resulted from the fact that most of the falling film flow rate have been evaporated when it goes through upper 4 tubes. For all the combinations of film flow rate and heat flux, the tube heat transfer coefficients of these two tubes exhibit a slightly ascending trend (at least not descending) with the increase in vapor velocity.

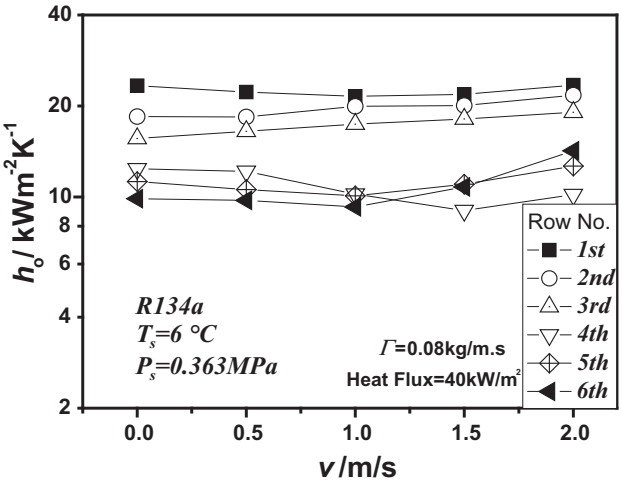

Fig. 15. Falling film heat transfer coefficients versus vapor flow at falling film flow rate 0.08 kg/m·s and heat flux 40 kW/m^2.

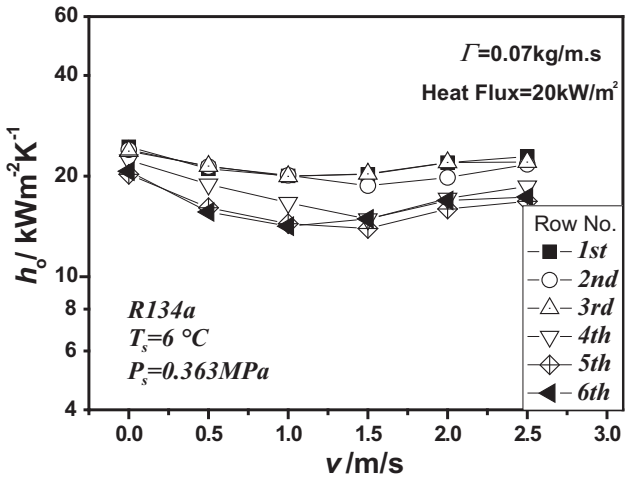

Fig. 13. Falling film heat transfer coefficients versus vapor flow at falling film flow rate 0.07 kg/m·s and heat flux 20 kW/m^2.

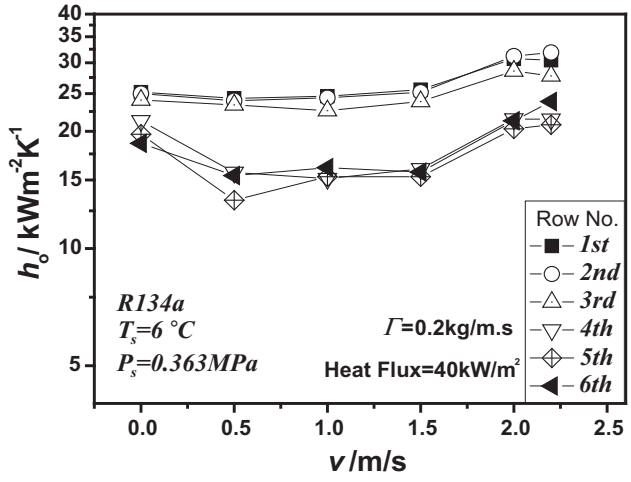

Fig. 16. Falling film heat transfer coefficients versus vapor flow at falling film flow rate 0.2 kg/m·s and heat flux 40 kW/m^2.

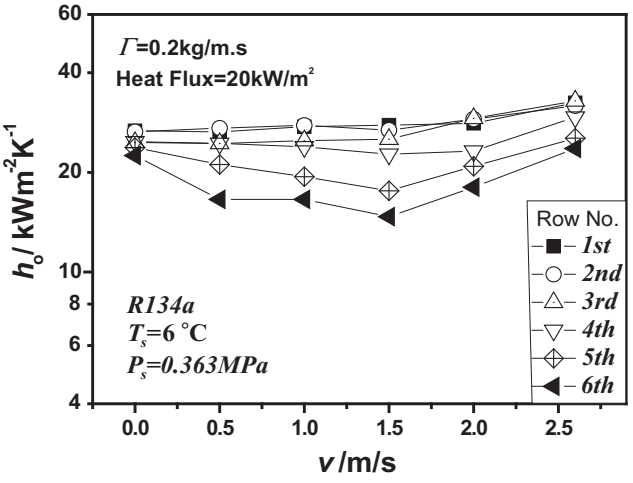

Fig. 14. Falling film heat transfer coefficients versus vapor flow at falling film flow rate 0.2 kg/m·s and heat flux 20 kW/m^2.

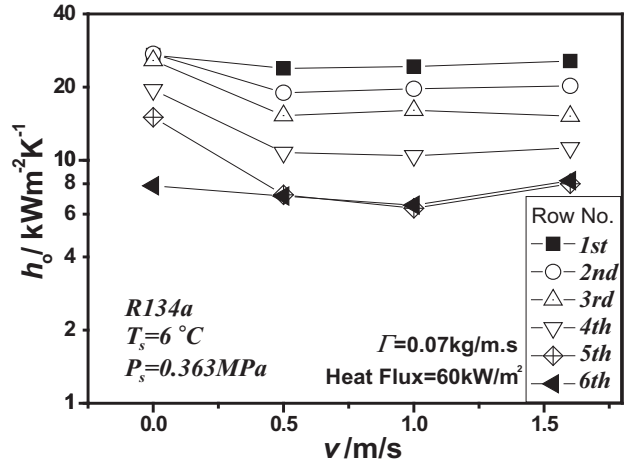

Fig. 17. Falling film heat transfer coefficients versus vapor flow at falling film flow rate 0.07 kg/m·s and heat flux 60 kW/m^2.

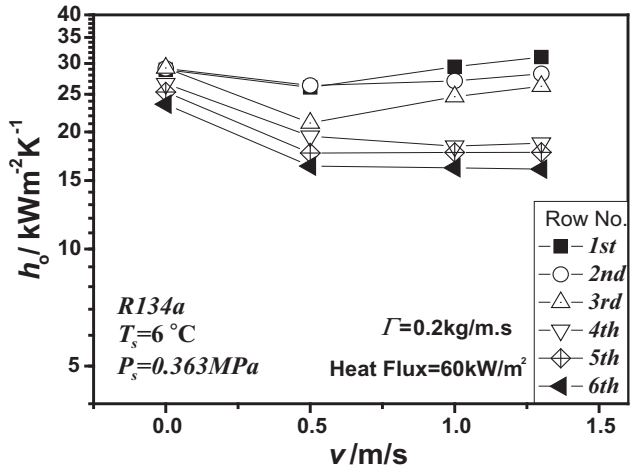

Fig. 18. Falling film heat transfer coefficients versus vapor flow at falling film flow rate 0.2 kg/m·s and heat flux 60 kW/m^2.

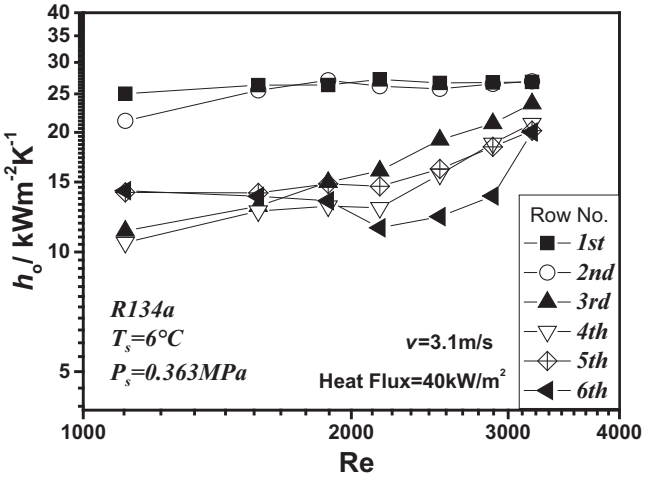

Fig. 19. Falling film heat transfer coefficients versus Re at vapor velocity 3.1 m/s and heat flux 40 kW/m^2.

(2) For the cases of heat flux equal to 20 kW/m^2 and flow rate of 0.07 and 0.2 kg/m·s, the tube heat transfer coefficients of the six ones are quite close to each other and have more or less similar variation trend with the increase of ascending vapor velocity. With the increment of vapor velocity, the evaporating coefficient decreases slightly firstly, at vapor velocity of 0.5–1.5 m/s reach the minimum and then increases with further increase in the vapor velocity. Such variation trend may be attributed to the film thickness change or sliding effects caused by the ascending vapor flow.

(3) With the increase in heal flux (q = 40, 60 kW/m^2), the deviations of tube heat transfer coefficients of the six tubes increase. However, the coefficients of the upper 1st, 2nd and 3rd tubes are always close to each other, probably because for the tested flow rates, 0.07, 0.08, and 0.2 kg/m·s, these three tubes always have enough liquid film to cover their surfaces.

(4) At the vapor velocity of 3.1 m/s and heat flux 40 kW/m^2 (seen Fig. 19), with the increment of Re from 1115 to 3191, the increase of heat transfer coefficients of the 1st and 2nd tube are very mild, probably because enough liquid film flow rate are guaranteed in the entire Re range for the upper two tubes; However for the other 4 tubes, the increasing trend is more significant. This can be understood that at lower film Reynolds number partial dry-out may occur. For the middle several tubes, from Re equal to 1115–3191 the increase ratio of tube heat transfer coefficient may be as large as two.

(5) Generally speaking, as far as the absolute values and variation trend are concerned, the 6 tubes studied can be divided into three groups, the upper two tubes, the bottom two tubes and the tubes of the middle part. As indicated above, the upper two tubes always have the same behavior, characterized by high heat transfer coefficients, not very sensitive to vapor velocity and film Reynolds number. Because the falling film is sufficient for evaporation, the film flow rate effect on the heat transfer coefficient is almost negligible for the two tubes. Then comes the bottom two tubes, very low tube heat transfer coefficients and comparably quite sensitive to vapor velocity. It is speculated that the vapor velocity might cause liquid maldistribution outside the tube surface in the lower position and dryout occurs. The differences between coefficients of tube Nos. 3–4 depend on film flow rate, and higher flow rate makes their heat transfer coefficients close to each other.

6. Conclusions

In this paper, the falling film heat transfer coefficients are measured for a vertical tube bank with 6 tubes at different heat fluxes. The effects of ascending vapor velocity are experimentally studied with additional vapor supplied by a boiler fixed in the circulation of liquid refrigerant. The vapor velocity ranges from 0 to 3.1 m/s. The following general conclusions can be drawn:

(1) The overall heat transfer coefficient of the test tube in falling film is about 16% higher than pool boiling. Within the heat flux tested, the heat transfer coefficient of the evaporation is insensitive to heat flux.

(2) Falling film flow rate is an important factor to influence the evaporating heat transfer coefficient; generally, the heat transfer coefficient increase with the increment of film Re for the tubes in the lower position.

(3) In the parameter range tested, the effect of ascending vapor velocity on the tube heat transfer coefficients is very complicated, depending on tube position, heat flux, film flow rate and the vapor velocity. Both negative and positive effects are found. Generally speaking, positive effects are predominant for the two tubes in the top positions and higher vapor velocity.

(4) Within the range of ascending vapor velocity from near zero to 3.1 m/s, the variation of tube heat transfer coefficient at the same condition covers a wide range, from several percentage to about 120%. Considering that the additional vapor supplied by the boiler creates vapor velocity much larger than practical one in engineering falling film evaporator, the effect of vapor shear stress may be neglected in practical engineering design at lower vapor velocity.

Conflict of interest

None declared.

Acknowledgments

Research fund for National Natural Science Foundation of China (51306140), National Key Basic Research Program of China (973

Program) (2013CB228304), and Daikin Cooperation of Japan are greatly acknowledged.

References

[1] J.F. Roques, J.R. Thome, Falling films on arrays of horizontal tubes with R-134a, Part II: flow visualization, onset of dryout, and heat transfer predictions, Heat Transfer Eng. 28 (5) (2007) 415–434.
[2] M. Christians, J.R. Thome, Falling film evaporation on enhanced tubes, Part 1: experimental results for pool boiling, onset-of-dryout and falling film evaporation, Int. J. Refrig. 35 (2) (2012) 300–312.
[3] M. Christians, J.R. Thome, Falling film evaporation on enhanced tubes, Part 2: prediction methods and visualization, Int. J. Refrig. 35 (2) (2012) 313–324.
[4] J.R. Thome, Falling film evaporation: state-of-the-art review of recent work, J. Enhanc. Heat Transfer 6 (1999) 263–278.
[5] G. Ribatski, A.M. Jacobi, Falling-film evaporation on horizontal tubes – a critical review, Int. J. Refrig. 28 (5) (2005) 635–653.
[6] J. Fernández-Seara, Á.Á. Pardiñas, Refrigerant falling film evaporation review: description, fluid dynamics and heat transfer, Appl. Therm. Eng. 64 (1–2) (2014) 155–171.
[7] A.M. Abed, M. Alghoul, M.H. Yazdi, A.N. Al-Shamani, K. Sopian, The role of enhancement techniques on heat and mass transfer characteristics of shell and tube spray evaporator: a detailed review, Appl. Therm. Eng. 75 (2015) 923–940.
[8] S.A. Moeykens, Heat Transfer and Fluid Flow in Spray Evaporators with Application to Reducing Refrigerant Inventory, Iowa State University, 1994.
[9] D. Gstoehl, Heat Transfer and Flow Visualization of Falling Film Condensation on Tube Arrays with Plain and Enhanced Surfaces, Swiss Federal Institute of Technology, Lausanne, 2004.
[10] J.-F. Roques, J. Thome, Falling films on arrays of horizontal tubes with R-134a, Part I: boiling heat transfer results for four types of tubes, Heat Transfer Eng. 28 (5) (2007) 398–414.
[11] S.A. Moeykens, M.B. Pate, Spray evaporation heat transfer of R134a on plain tubes, ASHRAE Trans. 100 (2) (1994) 173–184.
[12] J.F. Roques, V. Dupont, J.R. Thome, Falling film transitions on plain and enhanced tubes, ASME J. Heat Transfer 124 (3) (2002) 491–499.
[13] D. Gstöhl, J. Thome, Visualization of R-134a flowing on tube arrays with plain and enhanced surfaces under adiabatic and condensing conditions, Heat Transfer Eng. 27 (10) (2006) 44–62.
[14] G. Ribatski, J.R. Thome, A visual study of R134a falling film evaporation on enhanced and plain tubes, in: 5th International Symposium on Multiphase Flow, Heat Mass Transfer and Energy Conversion, Xi'an, China, 2005.
[15] B. Ruan, A.M. Jacobi, L. Li, Effects of a countercurrent gas flow on falling-film mode transitions between horizontal tubes, Exp. Therm. Fluid Sci. 33 (8) (2009) 1216–1225.
[16] B. Cheng, W.Q. Tao, Experimental study of R-152a film condensation on single horizontal smooth tube and enhanced tubes, ASME J. Heat Transfer 116 (1) (1994) 266–270.
[17] V. Gnielinski, New equations for heat and mass transfer in turbulent pipe and channel flows, Int. Chem. Eng. 16 (1976) 359–368.
[18] W.T. Ji, D.C. Zhang, N. Feng, J.F. Guo, M. Numata, G. Xi, W.Q. Tao, Nucleate pool boiling heat transfer of R134a and R134a-PVE lubricant mixtures on smooth and five enhanced tubes, ASME J. Heat Transfer 132 (11) (2010) 11502.
[19] S.J. Kline, F.A. Mcclintock, Describing uncertainties in single-sample experiments, Mech. Eng. 75 (7) (1953) 3–9.
[20] S.M. Yang, W.Q. Tao, Heat Transfer, Higher Education Press, Beijing, 2006.
[21] W.T. Ji, D.C. Zhang, Y.L. He, W.Q. Tao, Prediction of fully developed turbulent heat transfer of internal helically ribbed tubes – an extension of Gnielinski equation, Int. J. Heat Mass Transfer 55 (4) (2012) 1375–1384.
[22] D.C. Zhang, W.T. Ji, W.Q. Tao, Condensation heat transfer of HFC134a on horizontal low thermal conductivity tubes, Int. Commun. Heat Mass Transfer 34 (8) (2007) 917–923.
[23] W.T. Ji, C.Y. Zhao, D.C. Zhang, Y.L. He, W.Q. Tao, Influence of condensate inundation on heat transfer of R134a condensing on three dimensional enhanced tubes and integral-fin tubes with high fin density, Appl. Therm. Eng. 38 (2012) 151–159.
[24] M. Habert, Falling Film Evaporation on a Tube Bundle with Plain and Enhanced Tubes, Ecocle Polytechnique Federale De Lausanne, 2009.